

REPORT DOCUMENTATION PAGE			Form Approved OMB No. 0704-0188
<p>Public reporting burden for this collection of information is estimated to average 1 hour per response, including the time for reviewing instructions, searching existing data sources, gathering and maintaining the data needed, and completing and reviewing the collection of information. Send comments regarding this burden estimate or any other aspect of this collection of information, including suggestions for reducing this burden, to Washington Headquarters Services, Directorate for Information Operations and Reports, 1215 Jefferson Davis Highway, Suite 1204, Arlington, VA 22202-4302, and to the Office of Management and Budget, Paperwork Reduction Project (0704-0188), Washington, DC 20503.</p>			
1. AGENCY USE ONLY (Leave blank)	2. REPORT DATE	3. REPORT TYPE AND DATES COVERED	
	17 June 1997	Progress/ Technical Report 30 Aug 96-30 Aug 97	
4. TITLE AND SUBTITLE	Progress/Technical Report through period 30 August 1996 - 30 August 1997 titled, "Feasibility of bottom classification with the Toroidal Volume Search Sonar (TVSS)"		5. FUNDING NUMBERS
6. AUTHOR(S)	Dr. Nicholas P. Chotiros		
7. PERFORMING ORGANIZATION NAMES(ES) AND ADDRESS(ES) Applied Research Laboratories The University of Texas at Austin P.O. Box 8029 Austin, Texas 78713-8029			
9. SPONSORING/MONITORING AGENCY NAME(S) AND ADDRESS(ES) Samuel Tooma, Code 7430 Naval Research Laboratory Building 1005 Stennis Space Center, MS 39529-5004		10. SPONSORING/MONITORING AGENCY REPORT NUMBER <i>NRL/CR/h430-- 97-0009</i>	
11. SUPPLEMENTARY NOTES			
12a. DISTRIBUTION/AVAILABILITY STATEMENT Approved for public release; distribution unlimited.		12b. DISTRIBUTION CODE	
13. ABSTRACT (Maximum 200 words) This is a progress report for the first year of work on bottom classification using tactical sensors. Data from a TVSS experiment in 1994, at deep and shallow sites, were provided by CSS and distributed by NRL/SSC. The data were processed and analyzed to provide calibration in a self-consistent manner and then to compute the magnitude of the normal incidence bottom reflection coefficient, which was then used to estimate bottom type. Difficulties due to clipping of the signal were detected and partially overcome. The results show the deep and shallow sites to be quite different with respect to bottom type. The TVSS system gain was too high for sediment classification purposes because it tends to clip the specular bottom reflected signal particularly over hard bottoms. A lower system gain setting is probably not an acceptable solution, therefore, it is suggested that a small proportion of pings be reserved for bottom classification purposes, perhaps every tenth ping, in which the source level is reduced by 20 dB.			
14. SUBJECT TERMS			15. NUMBER OF PAGES 1
			16. PRICE CODE
17. SECURITY CLASSIFICATION OF REPORT Unclassified	18. SECURITY CLASSIFICATION OF THIS PAGE Unclassified	19. SECURITY CLASSIFICATION OF ABSTRACT Unclassified	20. LIMITATION OF ABSTRACT

**Progress/Technical Report**

**Grant No. N00014-96-C-6025**

**30 August 1996 - 30 August 1997**

**Title: Feasibility of bottom classification with the Toroidal Volume**

**Search Sonar (TVSS)**

**By: Nicholas P. Chotiros**

**Abstract:**

This is a progress report for the first year of work on bottom classification using tactical sensors. Data from a TVSS experiment in 1994, at deep and shallow sites, were provided by Coastal Systems Station (CSS) and distributed by Naval Research Laboratory/Stennis Space Center (NRL/SSC). The data were processed and analyzed to provide calibration in a self-consistent manner and then to compute the magnitude of the normal incidence bottom reflection coefficient, which was then used to estimate bottom type. Difficulties due to clipping of the signal were detected and partially overcome. The results show the deep and shallow sites to be quite different with respect to bottom type. The TVSS system gain was too high for sediment classification purposes because it tends to clip the specular bottom reflected signal particularly over hard bottoms. A lower system gain setting is probably not an acceptable solution, therefore, it is suggested that a small proportion of pings be reserved for bottom classification purposes, perhaps every tenth ping, in which the source level is reduced by 20 dB.

**Introduction:**

Operations in littoral waters are very dependent on environmental conditions, which impact the performance of a number of systems including weapons and sonars. The properties of the seafloor will have a strong impact on sonar performance and on the detectability of mines. The long-term

objective is to investigate methods of extracting bottom sediment classification from acoustic signals generated by tactical unmanned underwater vehicle (UUV) systems, for the purpose of supporting mine countermeasures (MCM) mission needs, including sediment classification, mine burial and sonar detection performance prediction against bottom, proud and buried, mines. This is a component of the NRL Environmental Sensing Program using Tactical MCM Systems.

One source of data is the Toroidal Volume Search Sonar (TVSS). The TVSS consists of a pair of cylindrical arrays wrapped around a horizontal cylindrical body. One array projects a sound pulse in a plane perpendicular to the axis of the cylinder. A number of pulse types may be used including pulsed continuous wave (CW) and linear frequency modulation (LFM). The other is a receiving array that may be used to form multiple receiving beams in the same plane. Two types of receiving arrays are provided, ceramic and polymer. TVSS data contains bottom reflection and backscattering information that may be used for sediment classification and testing of existing acoustic models, particularly the model from Applied Physics Laboratory/University of Washington (APL/UW) which assumes a fluid bottom assumption and the model from Applied Research Laboratories, The University of Texas at Austin (ARL:UT) which uses Biot's theory. In this study, the emphasis will be on sediment classification from normal incidence bottom reflection measurement.

#### **Approach:**

The adopted approach is to extract relevant sediment properties directly from the acoustic signals received by the TVSS, without interfering with the normal operation of the system. Possible outputs include: sediment porosity, gas bubble content and bottom roughness, from which shear strength, mean grain size and other properties may be inferred. A modeling approach will be used to obtain relationships between acoustic signal attributes and sediment properties. Current elastic models of ocean sediments, in which the sediment is assumed to behave as an elastic solid, have very little connection to sediment

properties, such as grain size, porosity and shear strength. Echo strength, by itself, is an ambiguous indicator of sediment type, because a soft sediment containing gas bubbles can have a reflection loss that is comparable to a hard sediment, such as sand. A model that accurately represents the physical mechanisms is needed in order to properly interpret sediment acoustic signals. Biot's theory of acoustic propagation in porous media provides the foundation for such a model. When combined with signal processing techniques that are capable of extracting the necessary model inputs, a physically sound sediment classification process may be obtained.

Within the context of Biot's theory, it is expected that normal incidence reflection loss will be very sensitive to sediment porosity, which, in turn, is known to be related to shear strength and sediment grain size. However, the presence of gas in the sediment may affect the reflection loss and lead to erroneous porosity estimates. A method has been developed to identify the contribution of gas bubbles<sup>1</sup> to the acoustic signal, based on wavelet analysis. Bottom roughness may also reduce echo strength. The issue of bottom roughness and its effect on the acoustic echo has been modeled<sup>2</sup> using realistic sediment roughness spectra measured by Briggs.<sup>3</sup> Roughness is expected to reduce the normal incidence echo strength at higher frequencies, therefore spectral analysis may be used to look for its effects. It is proposed that these methods and models be combined into a comprehensive, physics based, sediment classification process and applied to the TVSS signals, as illustrated in Fig. 1.

#### **Accomplishments:**

This report addresses the feasibility of using TVSS data for bottom classification, particularly the ability to support the above mentioned models and signal processing methods. Taped data recorded from sea tests were used. Selected data sets were made available by the Coastal Systems Station (CSR) and distributed by the Naval Research Laboratory, Stennis Space Center (SSC).

Center (NRL/SSC). The data were from sea tests conducted, between 19 October and 20 November 1994, in two mutually exclusive sites<sup>4</sup> referred to as "shallow field" and "deep field". Data collection was made along straight tracks, in a North-South or East-West direction. The data set from each track was called a "run" and numbered consecutively. In each run, data were collected by pinging at regular intervals and recording the returned signals at each element in the receiving array, along with auxiliary data including vehicle position and heading. The data provided included approximately 10 pings of Run 1 and 100 pings of Run 6 on 8 November, and 10 pings of Run 4 on 9 November. All were taken with a 1 ms CW pulse, and a ceramic array. The received signals were subjected to a time varying gain (TVG) amplifier and band-pass filtering before being digitized and stored. Relevant and helpful information concerning the data collection were provided by Lisa Tubridy,<sup>5</sup>

CSR.  
CSS

A FORTRAN program was provided by CSR for reading the data and for beamforming. The program was ported to a Macintosh computer and recompiled using a FORTRAN compiler from Absoft. The resulting code was used to examine the raw data and generate beamformed data for display and analysis.

Three types of processes were considered for sediment classification purposes:

1. Normal incidence reflection loss measurement
2. Wavelet analysis
3. Power spectrum analysis

In this reporting period, the data were successfully decoded and normal incidence reflection loss measurements were accomplished. An example of the signal power spectrum an element in the receiving array is shown in Fig. 2. The power spectrum appears to be centered about an intermediate frequency (i.f.) of approximately 6 kHz. It is evident that the bandwidth is only 1 kHz, which consistent with the pulse 1 ms CW pulse used. Wider bandwidth data exist but

were not yet made available. The wavelet and power spectrum analyses will be deferred to the next reporting period because they require greater bandwidth. The steps leading to normal incidence reflection loss measurements and subsequent sediment classification are described as follows.

### **Calibration:**

In measuring the normal incidence reflection loss, the system calibration had to be established. This may be divided into two areas: the time varying gain (TVG) function, and non-time varying system calibration.

The TVG was measured from the system noise floor observable in the raw signal from each receiving element. An example is shown in Fig. 3. It was found that for the vast majority of the elements, the noise floor, hence the TVG, may be approximated by a function of the form:

$$\begin{aligned} \text{TVG} &= 35 * \text{LOG}(\text{RANGE}) + 2 * \text{ALPHA} * \text{RANGE} ; \text{ if } \text{RANGE} > 60 \text{ m} \\ &= 35 * \text{LOG}(60) + 2 * \text{ALPHA} * 60 \quad ; \text{ if } \text{RANGE} \leq 60 \text{ m} \quad (1) \end{aligned}$$

where RANGE is calculated from elapsed time assuming a sound speed of 1500 m/s, and ALPHA is the attenuation, assumed to be 0.024 dB/m.

The non-time varying system calibration may be obtained from the echo level of a signal reflected by a flat and lossless surface, such as the sea surface under calm conditions. The data from the shallow site were inspected for this purpose but the raw signals were found to be clipped. This was a significant set back since all of the data processing schemes and the calibration procedure require that all processes between signal transmission and analog-to-digital conversion be linear. Examples of the signal levels from every tenth element in ping 410 of 08nov94 Run 6, from the shallow site, are shown in Fig. 4 as an illustration. The plots show that the signal levels from all elements saturating at a value of 84 dB referenced to the digital unit, which is indicative of clipping. In

this case the TVSS was at almost exactly mid-depth. The signal level at the upward looking elements (1 to 30 and 89 to 120, dashed lines) reached saturation slightly before those of the downward looking elements (31 to 90, solid lines). At the range marked "A", the signal levels from all elements hit saturation. These are indications of severe clipping. On inspection, the raw data samples do not appear to be clipped, as shown in Fig. 5. Therefore, it is concluded that the clipping must have occurred in the amplifier stages leading up to the bandpassfilter, as illustrated in Fig. 6. The clipping may have occurred at points marked "a", "b" or "c". The band-pass filtering would remove the higher harmonics of the clipped signal and restore its sinusoidal shape giving a false appearance of an undistorted signal.

The raw signals from the deep site were less severely clipped, as shown in Fig. 7. In this case, the TVSS was closer to the surface than the bottom. The surface echo arrived at the upward looking elements at a range of 72 m and saturated at a level of 86 dB, which is 2 dB higher the 84 dB at 17 m in the shallow site. This indicates that the saturation limit changes as function of TVG gain, and suggests that the clipping must have occurred in either the pre-amplifier before the TVG stage, or the earlier stages of a multi-stage TVG amplifier. The signal levels of the bottom echo, arriving at a range of 117 m, appear to be just below the saturation level.

The surface echo from the deep site was examined more closely. In Fig. 8(a) the signal levels from 4 elements are shown. The plots indicate that not all signals were saturated. The greatest degree of saturation occurred at range "a". There was a smaller degree of saturation at "b", and none at "c". The signals from the three ranges were plotted as a function of element number, and corresponding radial angle, in Fig. 8(b). It is evident that, at "a" all the upward looking elements experienced saturation, but at "c" only a few near the apogee were weakly saturated. Therefore, the curve at "c" may be used as a template of the shape of the surface echo curve. The unsaturated signal curve at "a" may be estimated by projecting the "a" curve upwards to match the shape of the "c"

curve. By this method, it was estimated that the peak levels at the 30 elements nearest to the upward vertical were reduced by 17 dB due to clipping. These same elements are used to form the upward looking beam, therefore the beamformed signal must also be reduced by the same amount.

The raw data were beamformed and the resulting intensity plots are shown in Fig. 9. The magnitude of the reflection coefficient R, in decibels, may be calculated according to the following equation:

$$R = RL - TVG - CAL + 20 \cdot \text{LOG}(2 \cdot \text{RANGE}) + 2 \cdot \text{RANGE} \cdot \text{ALPHA} \quad (2)$$

where RL is the received level of the beamformed signal, in decibels referenced to one digital unit, at the peak of the normal incidence echo; TVG is given by Eq. (1), and RANGE is in meters; CAL is the non-time varying system calibration. Given that the surface was calm at the deep site, during 09nov94 Run 4, as indicated by the lack of surface backscatter on either side of the specular reflection in Fig. 9(a), the surface reflection loss must have been very close to zero decibels. Using Eq. (2), the surface echo from the deep site was used to invert for the value of CAL, adjusting for the 17 dB reduction due to clipping. CAL includes the source level of the projected 1 ms CW pulse, the sensitivity of the receiving elements, amplifier and beam former gains, and the A-D conversion factor. The result was

$$\text{CAL}=93 \text{ dB} \quad (3)$$

This value of CAL was applied to the data from both sites.

#### **Reflection loss measurement:**

Applying Eq. (2) to the direct bottom echo from the deep site, the value of R was found to be -28.2 dB, as shown in Fig. 9(a). The surface-bottom multiple and its inverse gave R values of approximately -42 dB. In theory, these values

should have been the same as that of the direct bottom reflection because the surface reflection is lossless. The discrepancy of -14 dB was most likely due to shadowing by the TVSS vehicle. In both the surface-bottom multiple and its inverse path, the sound must travel through the TVSS vehicle and suffer a shadowing loss. Due to the reciprocal nature of the two paths, the shadowing losses are expected to be identical.

Applying Eq. (2) to the direct surface and bottom echoes from the shallow site without correcting for clipping, the values of R obtained were -32 dB and -30 dB, respectively. The surface was not calm, as evidenced by significant backscatter on either side of the specular reflection, and furthermore the surface echo in the specular direction appears to be centered a point below the air-water interface, probably due to the wake of the towing ship, making the surface reflection useless for calibration purposes and difficult to interpret in any meaningful way. The bottom echo was certainly clipped as indicated in the element signal levels of Fig. 4. The clipping was more severe than that of the surface in the deep site, which was estimated to have been reduced by 17 dB. Therefore, the magnitude of the bottom reflection coefficient at the shallow site is estimated to be at least 17 dB greater than uncorrected value of -30 dB, which makes it greater than -13 dB.

### **Sediment classification:**

A model, based on Biot's theory of acoustic propagation in porous media, had been developed earlier, primarily for the modeling of acoustic bottom backscatter. It also models reflection coefficient as a function of grazing angle. The model, named BOGGART,<sup>6</sup> currently in version 3, contains empirical relationships that may be used to estimate the Biot parameters, including porosity, from grain size and to compute values of R. Resulting plots of R as a function of porosity and grain size, are shown in Fig. 10 (a) and (b), respectively. The grain size is given in phi units, defined as the negative of log base 2 of the grain diameter in millimeters. The R values from the deep and shallow sites

indicate very different bottom types. From the curve in Fig. 10 (a), the estimated porosity of the shallow site is 50% or less, indicating a bottom that is hard. It is not possible to be more precise due to clipping of the signal. The porosity of the deep site is estimated to be 90%, which indicates a very soft bottom. From Fig. 10 (b), the indicated mean grain sizes are 3 or less in phi units for the shallow site, which covers a wide variety of sands, and almost 10 phi for the deep site, which is a very soft clay.

### **Conclusions:**

Bottom classification from the TVSS complements the work planned by other participants, including the development of bathymetric algorithms (NRL and Scripps), backscatter image generation and processing (NRL, WHOI and Scripps), and sediment backscatter model parameter estimation (NRL and APL/UW), and system performance estimation (CSS and NRL). This is a progress report for the first year. Data from a TVSS experiment in 1994, from a deep and a shallow site, were provided by CSS and distributed by NRL/SSC. The data were processed and analyzed to provide calibration in a self-consistent manner and then to compute the magnitude of the normal incidence bottom reflection coefficient, which was then used to estimate bottom type. The above results show that limited bottom classification was accomplished. Difficulties due to clipping of the signal were detected and partially overcome. The results show the deep and shallow sites to be quite different with respect to bottom type. The deep site is estimated to have a very soft clay bottom, in which a mine will bury on impact, while the shallow site had a sandy bottom, in which a mine will not likely bury on impact, but may later become buried due to scouring. The TVSS system gain was presumed to be optimized for target detection, but it was too high for sediment classification purposes because it tends to clip the specular bottom reflected signal particularly over hard bottoms. A lower system gain setting is probably not an acceptable solution, because it may degrade mine detection performance. Therefore, it is suggested that a small proportion of pings be reserved for bottom classification purposes,

perhaps every tenth ping. In these pings, the source level should be reduced by 20 dB.

### **Acknowledgments:**

Thanks are due to Lisa Tubridy, CSS, for supporting information concerning the TVSS, to Maria Kalcic, NRL/SSC, and Darrel Jackson, APL/UW, for very useful discussions. Data processing at ARL:UT was performed by Adrienne Mautner and Frank Boyle. This work is supported by the Naval Research Laboratory, Stennis Space Center, Sam Tooma, chief scientist.

### **List of Figures:**

- Figure 1. Illustration of bottom classification with downward looking subset of TVSS beams
- Figure 2. Example of signal power spectrum
- Figure 3. Best fit TVG function to the noise floor of raw signal from a receiving element.
- Figure 4. Signal levels of every tenth element from ping 410 of 08nov94 Run 6, shallow site
- Figure 5. Example of recorded raw signal from element 10 from ping 410 of 08nov94 Run 6, shallow site, showing (a) the whole direct signal and (b) a close up of the saturated region
- Figure 6. The receiver block diagram showing points (a, b and c) where signals were likely clipped
- Figure 7. Signal levels of every tenth element from ping 10 of 09nov94 Run 4, deep site
- Figure 8. Surface echo at the deep site, showing (a) signal levels from four elements as a function of range, and (b) signal levels at three ranges (a, b, and c) as a function of element number, and radial angle, referenced to 0° at element 120.

Figure 9. Intensity plots of beamformed data from (a) ping 11 of 09nov94 Run 4, deep site, and (b) ping 499 of 08nov94 Run 6, shallow site

Figure 10. Reflection loss predictions by BOGGART v.3 as functions of (a) porosity and (b) grain size

---

**References:**

- 1 Russel D. Priebe, N. P. Chotiros, Donald J. Walter, Douglas N. Lambert, Gas bubble recognition by wavelet analysis and echo-sounder signals. Proc. Workshop on Modeling Methane-Rich Sediments of Eckernförder Bay, Eckernförder, 26-30 June, 1995.
- 2 N. P. Chotiros, Reflection and Reverberation in Normal Incidence Echo-Sounding. *J. Acoust. Soc. Am.* 96(5), 2921-9, November 1994.
- 3 K. B. Briggs, Microtopographical Roughness of Shallow-Water Continental Shelves. *IEEE J. Oceanic Eng.*, 14(4), 360-367, October 1989.
- 4 CSS Memorandum, "Environmental test report for high area rate reconnaissance test conducted 19 October through 20 November 1994," Code 3310, 20 December 1994.
- 5 Memo from Lisa Tubridy, CSS, to Charles Walker, NRL/SC, "High Area Rate Hunter (HARH) Toroidal Volume Search Sonar (TVSS) data," 25 August 1995.
- 6 Frank A. Boyle and Chotiros, Bottom Grain Gas and Roughness Technique (BOGGART) Version 3.0: Bottom Backscatter Model User's Guide. Technical Report No. (TR-96-10), Applied Research Laboratories, The University of Texas at Austin, 4 June 1996.

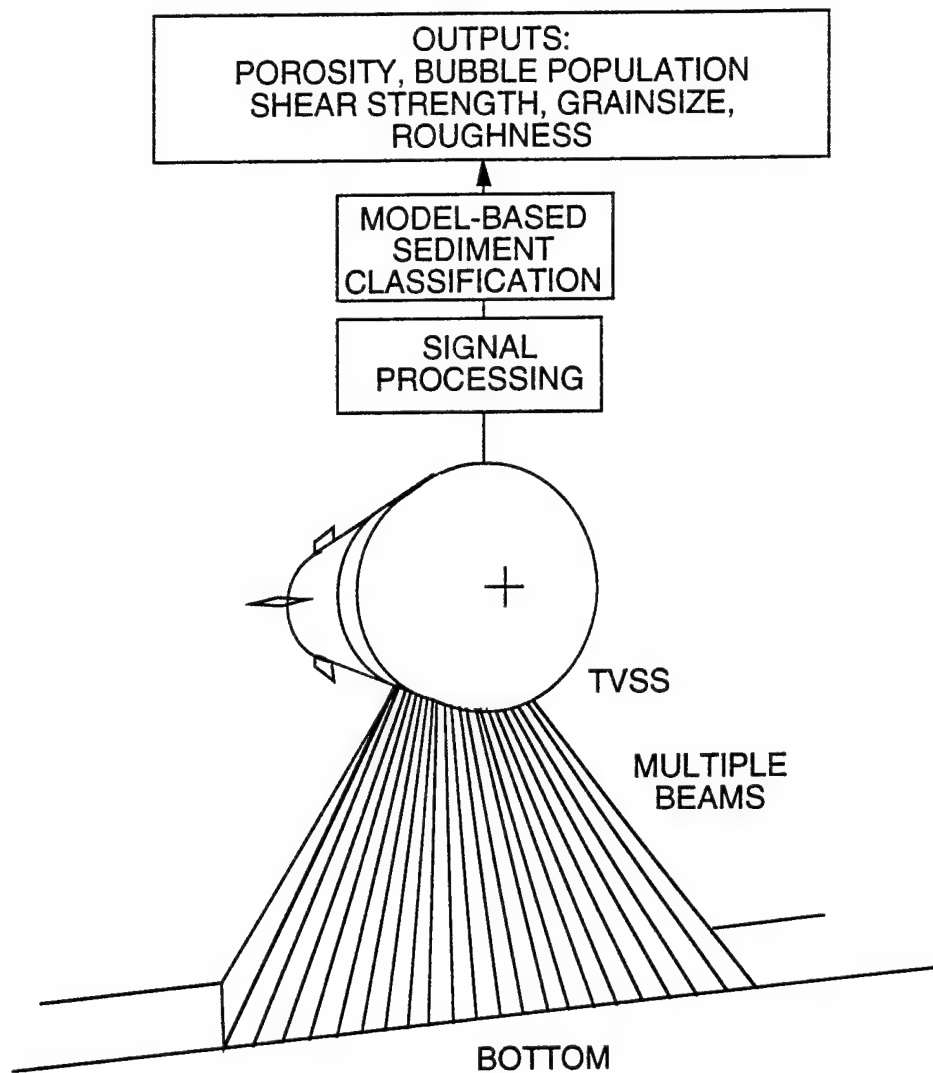


Figure 1. Illustration of bottom classification with downward looking subset of TVSS beams.

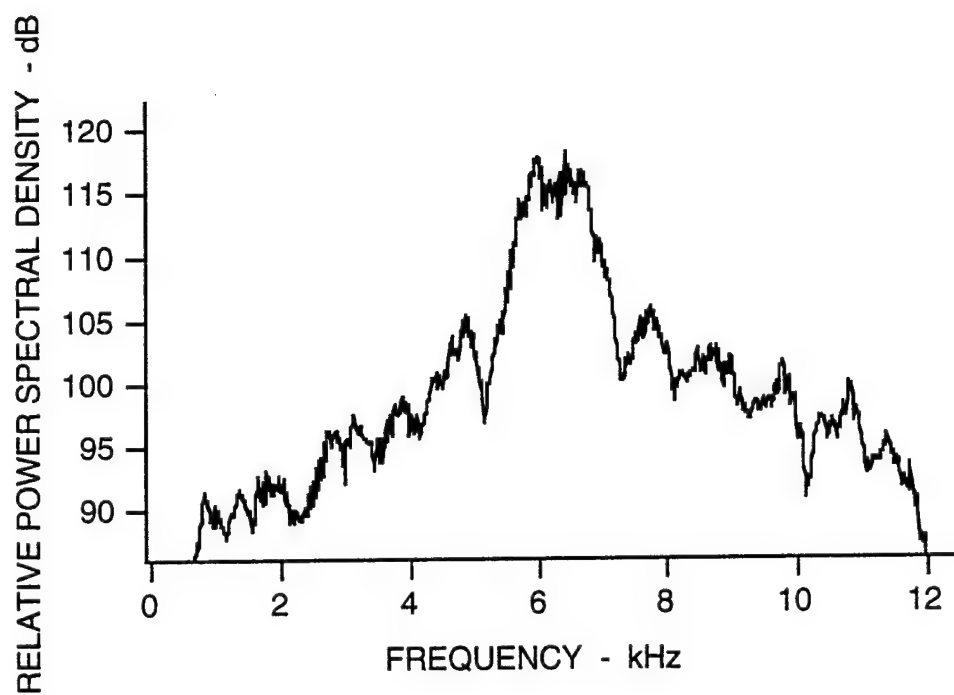


Figure 2. Example of signal power spectrum.

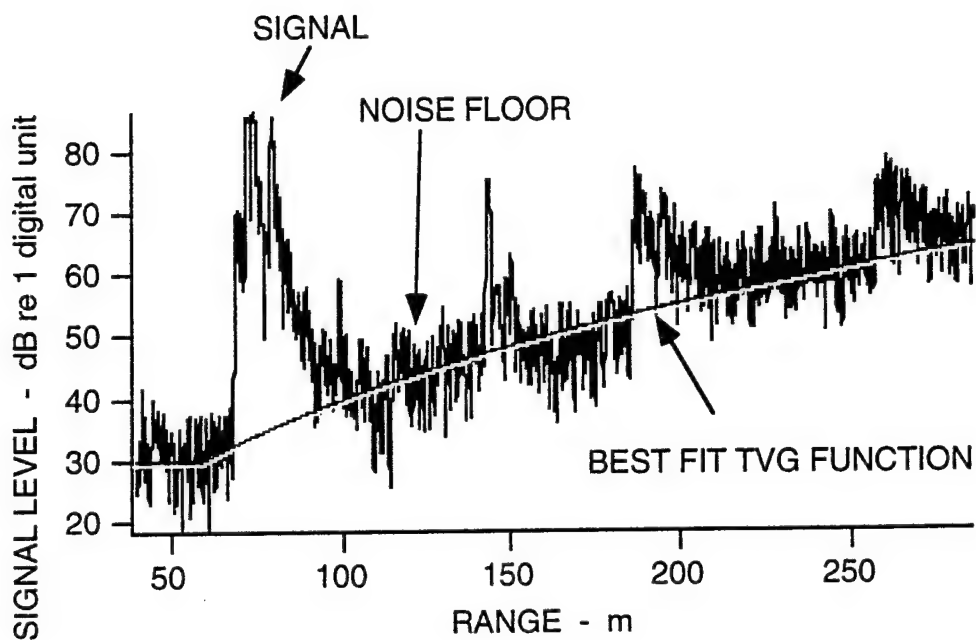


Figure 3. Best fit TVG function to the noise floor of raw signal from a receiving element.

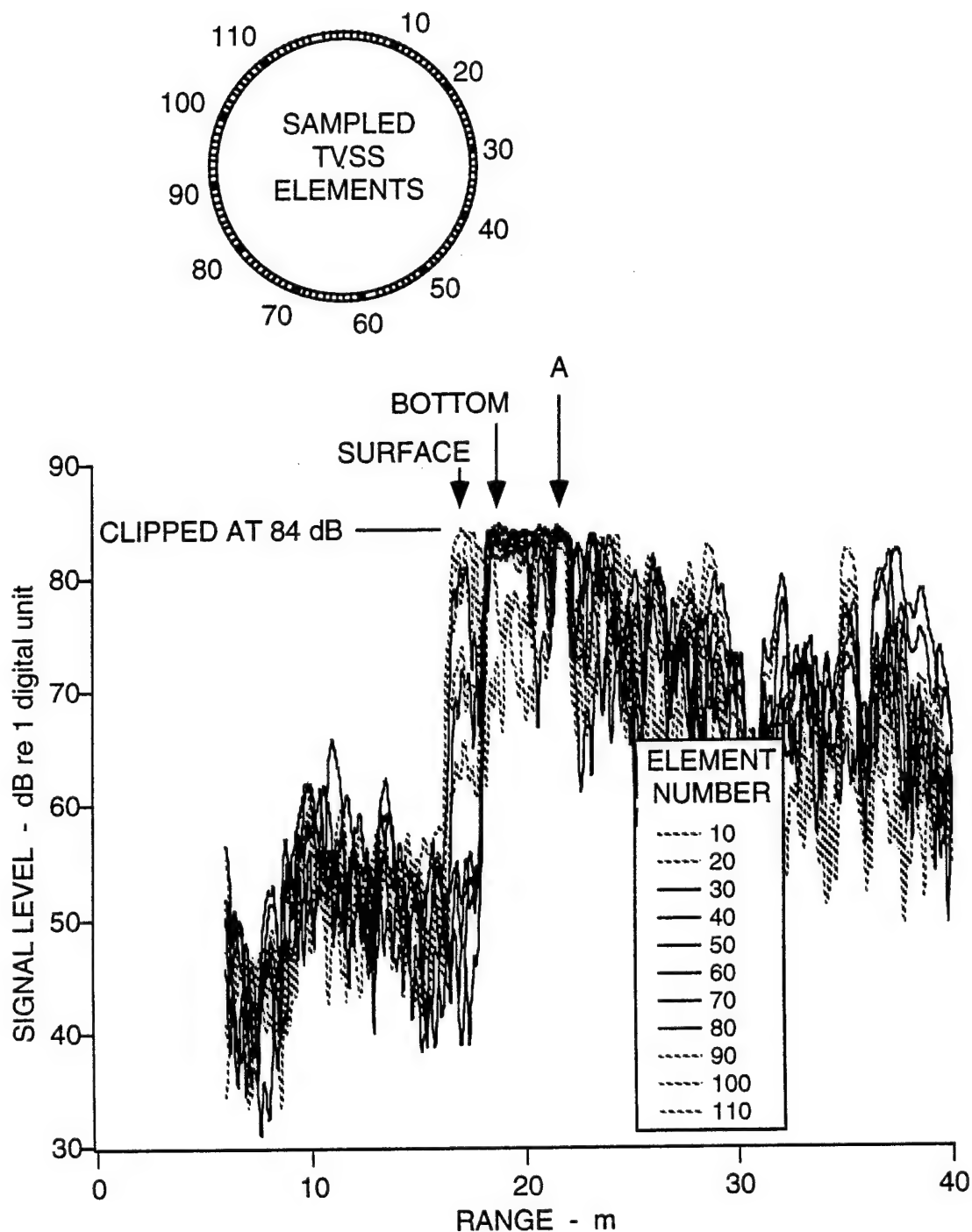


Figure 4. Signal levels of every tenth element from ping 410 of 08nov94 Run 6, shallow site.

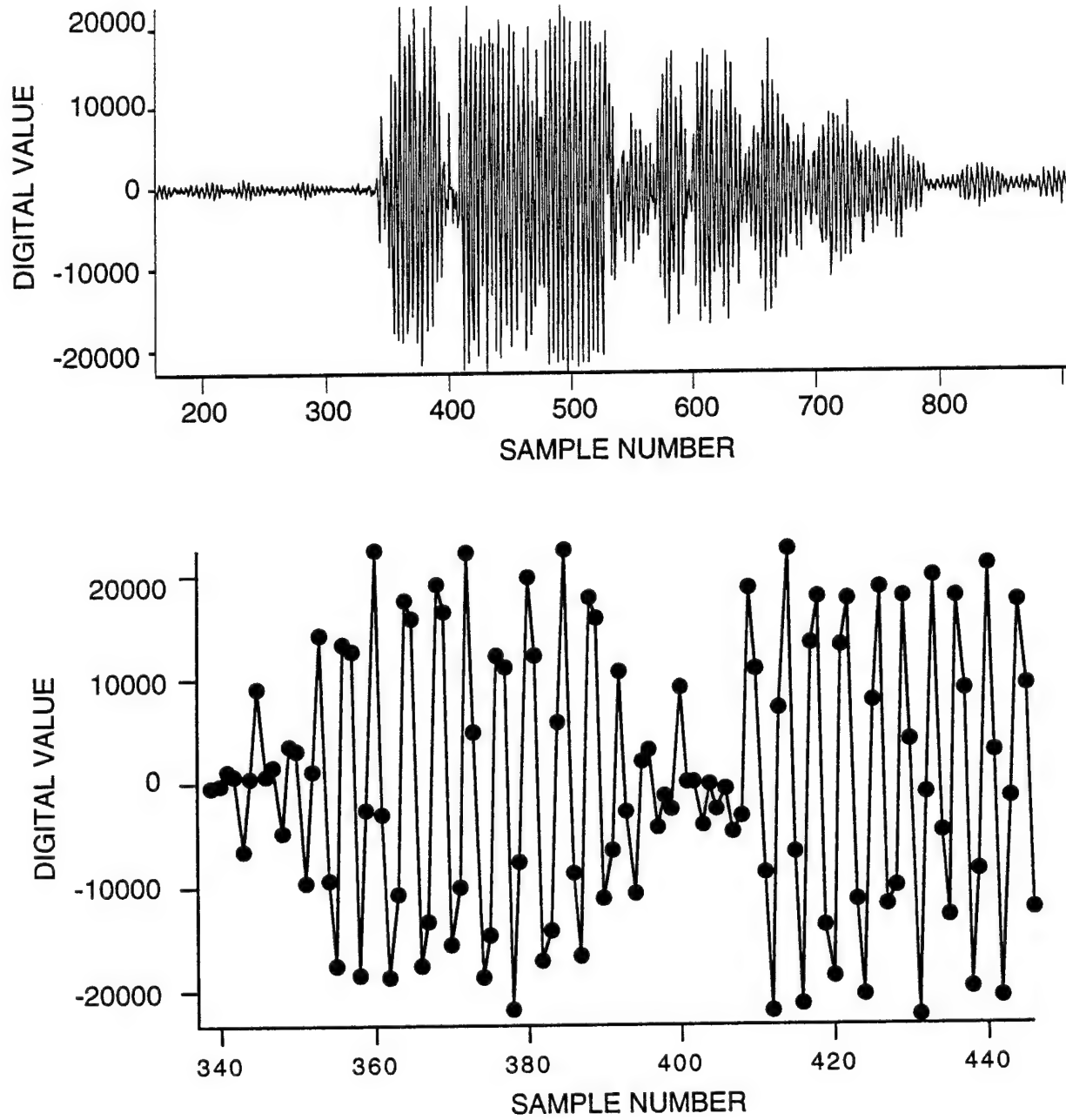


Figure 5. Example of recorded raw signal from element 10 from ping 410 of 08nov94 Run 6, shallow site, showing (a) the whole direct signal and (b) a close up of the saturated region.

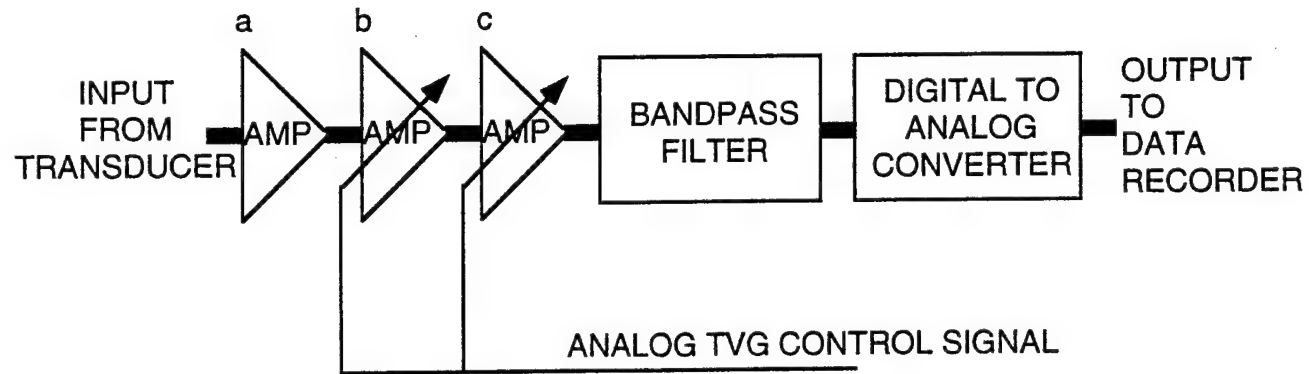


Figure 6. The receiver block diagram showing points (a, b and c) where signals were likely clipped.

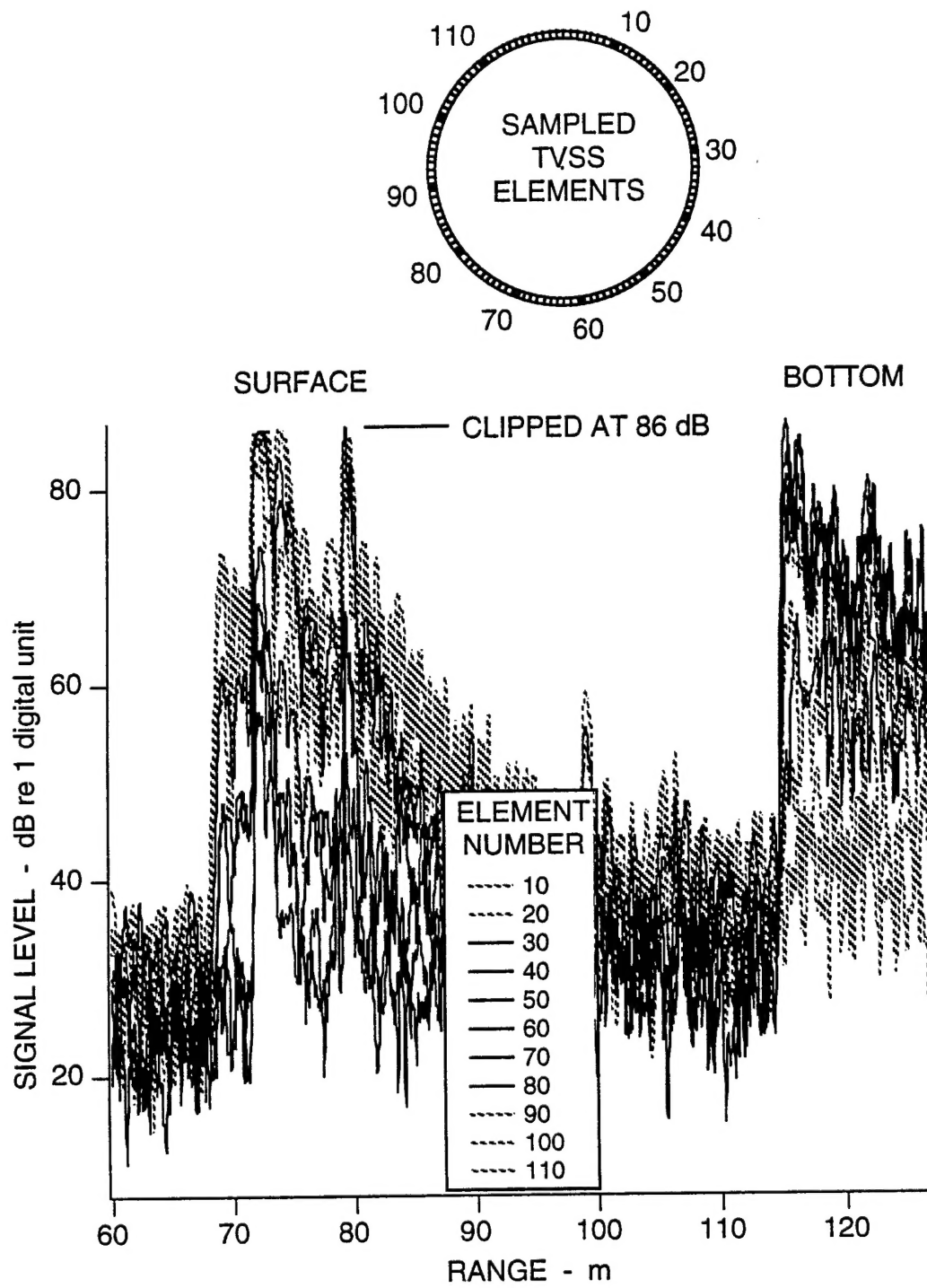


Figure 7. Signal levels of every tenth element from ping 10 of 09nov94 Run 4, deep site.

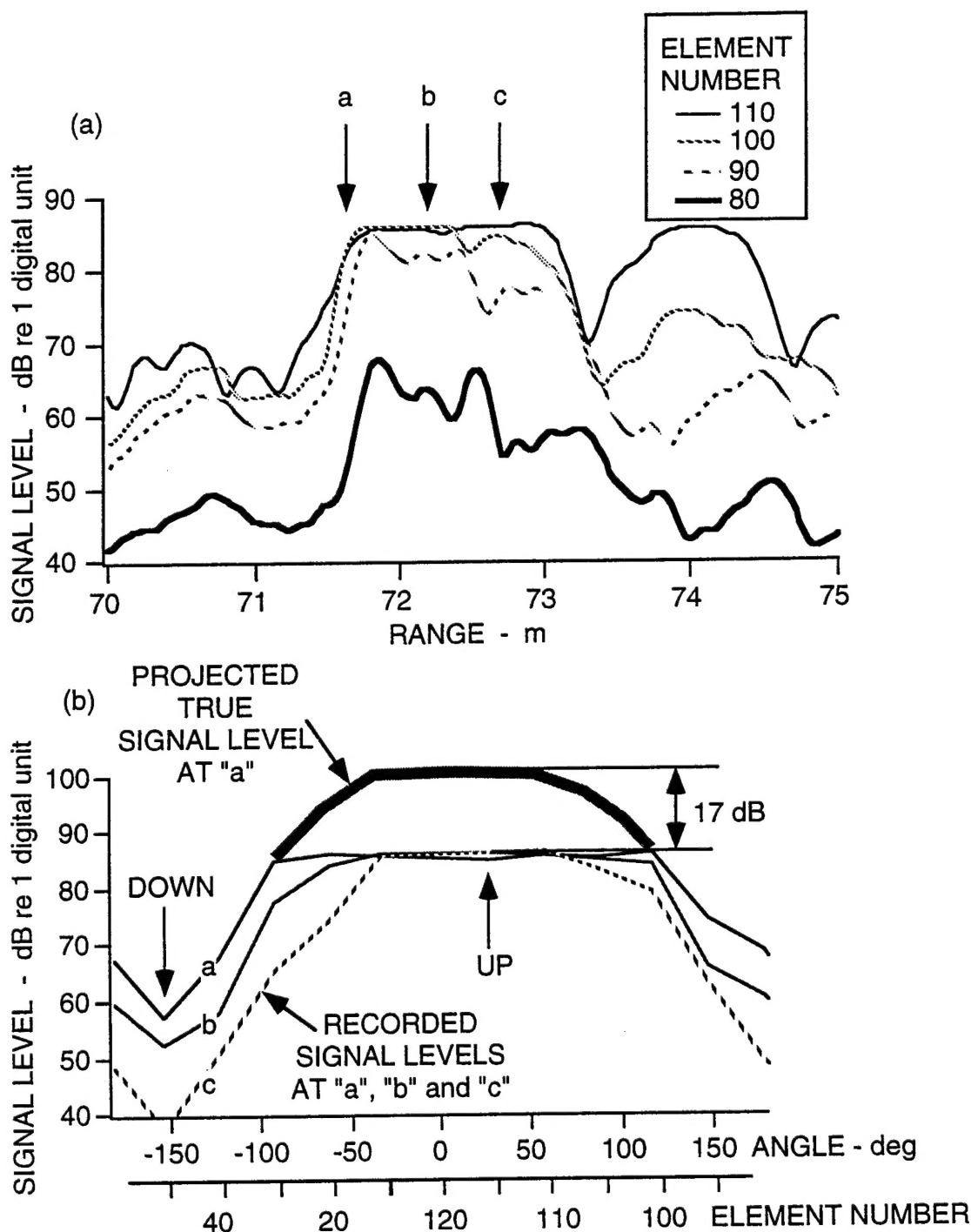


Figure 8. Surface echo at the deep site, showing (a) signal levels from four elements as a function of range, and (b) signal levels at three ranges (a, b, and c) as a function of element number, and radial angle, referenced to  $0^\circ$  at element 120.

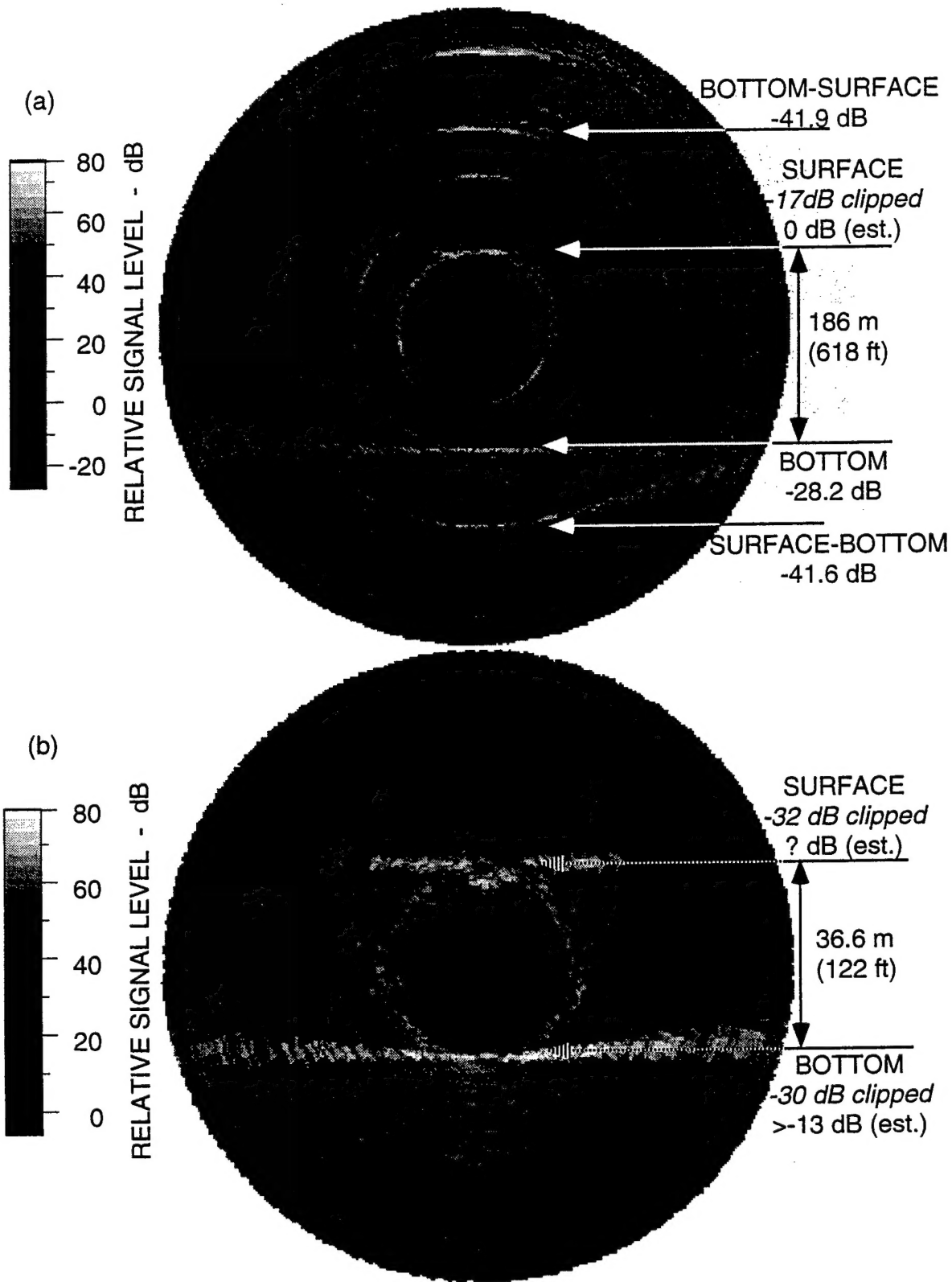


Figure 9. Intensity plots of beamformed data from (a) ping 11 of 09nov94 Run 4, deep site, and (b) ping 499 of 08nov94 Run 6, shallow site.

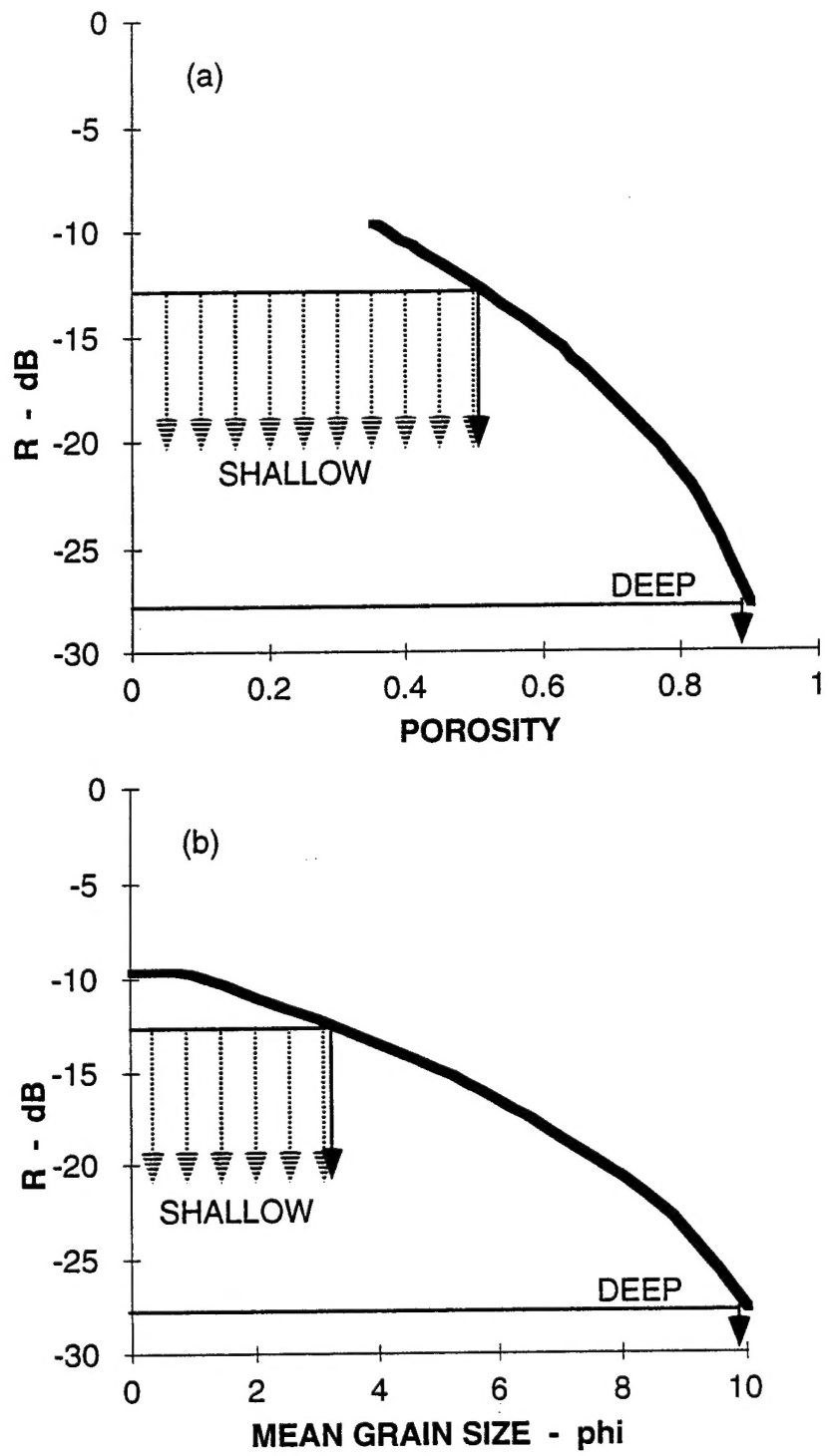


Figure 10. Reflection loss predictions by BOGGART v.3 as functions of (a) porosity and (b) grain size.